B110

Wave Attenuation by *Rhizophora* Mangroves: An Integrated Laboratory and Numerical Investigation

〇Yu-Lin TSAI, Che-Wei CHANG, Nobuhito MORI

Employing nature-based solutions to protect shorelines from natural hazards has been getting more attention in recent decades. This study investigated the *Rhizophora* mangrove-induced resistance to water waves using a fully nonlinear Boussinesq model. Adopting the perturbation method, the vegetation module is developed, accomplishing the drag and inertia terms due to vegetation with the vertical distribution of the *Rhizophora* mangrove tree and its prop roots. The relationship of the drag and inertia coefficients with Reynolds (Re) and Keulegan–Carpenter (KC) numbers proposed by Chang et al. (2022; doi: 10.1029/2022jc018653) was also investigated to quantify the applicable ranges of the proposed relationships in terms of wave attenuation on variant water depths.

1. Introduction

Vegetation has a protective function against coastal hazards and also been recognized as a green infrastructure (i.e., nature-based solutions) for coastal hazard mitigation. One notable coastal vegetation is mangroves, which was found to protect coastal communities from tsunamis (Danielsen et al., 2005). Hence, more attention has been paid in the recent two decades. Though the shape of mangroves' roots (i.e., Maza et al., 2019; Chang et al., 2022) has been considered in the lab experiments, its effect on wave modeling has not been investigated clearly, especially in the phase- resolving regime. Thus, this study develops a vegetation module onto a fully nonlinear Boussinesq wave model for wave attenuation modeling. Wave attenuations by *Rhizophora apiculate* mangroves are presented in this study.

2. Methodology

This study implements the vegetation module onto the fully nonlinear Boussinesq wave model (FUNWAVE), which was developed by Shi et al. (2012) and is accurate to O(μ^2) in the wave dispersive effect. Using the perturbation approach, the horizontal velocities $\boldsymbol{u}(z)$ can be expanded as

$$\boldsymbol{u}(z) = \boldsymbol{u}_{\boldsymbol{\alpha}} + (z_\alpha - z)\nabla\big(\nabla\cdot(h\boldsymbol{u}_{\boldsymbol{\alpha}})\big) + \frac{1}{2}(z_\alpha^2 - z^2)\nabla(\nabla\cdot\boldsymbol{u}_{\boldsymbol{\alpha}}) \tag{1}$$

where $\boldsymbol{u}_{\boldsymbol{\alpha}}$ is the horizontal velocity at the reference level z_α, z is the vertical location, and h is the still water depth. Introducing the expanded horizontal velocities to the dissipation term, the full integration approach is proposed here:

$$\boldsymbol{R_V} = -\frac{N}{2(h+\eta)}C_D\int_{-h}^{\min(h_v-h,\eta)}\boldsymbol{u}|\boldsymbol{u}|dA_{tree} - \frac{N}{(h+\eta)}C_M\int_{-h}^{\min(h_v-h,\eta)}\frac{\partial\boldsymbol{u}}{\partial t}dV_{tree} \tag{2}$$

in which, N is the forest density, (C_D,C_M) are drag and inertia coefficients, t denotes time, η is the free surface elevation, h_v is the stem height, and (dA_{tree},dV_{tree}) are the projected area and volume varied along the z-axis. Here, the vegetation-induced resistance is considered as momentum dissipative drag and inertia force terms. Similar dissipation term was introduced by Chakrabarti et al. (2017), but we further include the inertia force term in this study. The visualization of the approach with the conventional method is presented in **Figure 1**.

3. Results and Discussions

Wave attenuation by mangroves is tested following the experimental setup of Chang et al. (2022). **Figure 2** shows the mangrove tree, representing the nineteen-year-old *Rhizophora apiculate* mangrove in Vietnam. The computational domain is 61.5 m long with the sponge layers at the two ends. However, as the linear wavemaker is employed, an artificial 3:100 slope is added to generate waves smoothly (Chakrabarti et al., 2017). The width of mangrove areas is 4.07 m. The forest density is 29.4 stem/m^2, the diameter of the breast height is 1.0 cm, the height of prop roots is 13.5 cm, and the stem height of mangroves is 19.5 cm.
Wave attenuation due to mangroves with ±50% drag and inertia coefficient formulations is shown in **Figure 3**. The bottom friction is included (i.e., the Manning's coefficient is 0.013). The wave period is 1.7 s, and the still water depth is 17 cm. In the simulations, the drag and inertia coefficients are spatially varied according to the Reynolds (Re) and Keulegan-Carpenter (KC) numbers. We also found that the simulated wave attenuation varies more significantly when closer to the end of the mangrove forest.

4. Conclusion

This study has developed a vegetation module onto a fully nonlinear Boussinesq wave model (FUNWAVE-VEG). The wave attenuations due to mangroves were explored, and the mangrove tree's geometry was considered in the simulations. The trend of simulated attenuation fits the lab measurements, but the variations become larger when closer to the end of the mangrove forest. By presenting this numerical model package, we hope to pay the way for simulating wave attenuations considering the complete vegetation shape.

References

Chakrabarti et al. (2017). JGR-Oceans.

Chang et al. (2022). JGR-Oceans.

Dalrymple et al. (1984). JWPCOE.

Danielsen et al. (2005). Science.

Shi et al. (2012). Ocean Modelling.

Maza et al. (2019). Advances in Water Resources

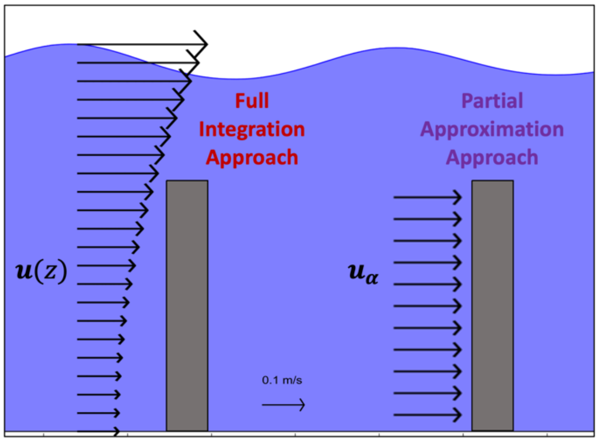

Figure 1: Sketch of vegetation-induced resistance to water waves: (left) the full integration approach used in this study; (right) the conventional method.

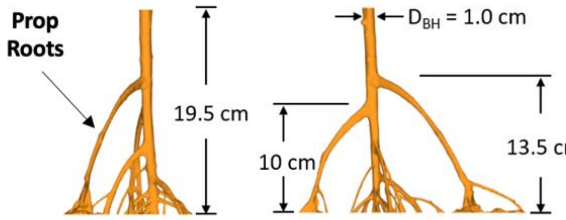

Figure 2: Replicated *Rhizophora apiculate* mangrove model in the lab experiment.

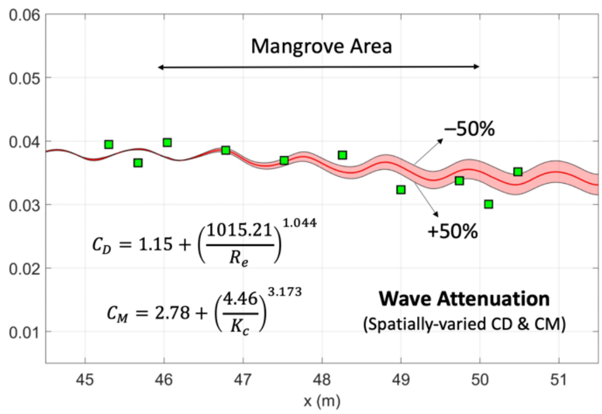

Figure 3: Wave attenuation by mangroves on the still water depth of 17 cm with input of the CD-Re and CM-KC relations. The y-axis is the significant wave height.